Published in final edited form as:
Invest Ophthalmol Vis Sci. 2009 May ; 50(5): 2368–2375. doi:10.1167/iovs.08-2696.

Defining the Residual Vision in Leber Congenital Amaurosis Caused by *RPE65* Mutations

Samuel G. Jacobson[1], **Tomas S. Aleman**[1], **Artur V. Cideciyan**[1], **Alejandro J. Roman**[1], **Alexander Sumaroka**[1], **Elizabeth A. M. Windsor**[1], **Sharon B. Schwartz**[1], **Elise Heon**[2], and **Edwin M. Stone**[3]

[1]Department of Ophthalmology, Scheie Eye Institute, University of Pennsylvania, Philadelphia, Pennsylvania

[2]Department of Ophthalmology and Vision Sciences, The Hospital for Sick Children, University of Toronto, Toronto, Ontario, Canada

[3]Howard Hughes Medical Institute and Department of Ophthalmology, University of Iowa Hospitals and Clinics, Iowa City, Iowa.

Abstract

PURPOSE—To quantify the residual vision in Leber congenital amaurosis (LCA) caused by *RPE65* mutations.

METHODS—Patients with *RPE65*-LCA (n = 30; ages, 4–55) were studied using electroretinography (ERG), full-field stimulus testing (FST), kinetic and static threshold perimetry, and optical coherence tomography (OCT).

RESULTS—All patients with *RPE65*-LCA had abnormal ERGs even at the youngest ages. There were no detectable rod ERGs and only reduced cone ERGs. By chromatic FST, however, 59% of patients had measurable rod- and cone-mediated function. The remaining 41% had only cone-mediated function. Extent of kinetic fields varied widely in the first two decades of life but, by the end of the third decade, there was very little measurable field. Regional patterns of visual loss were evident using dark-adapted static threshold perimetry. The mildest dysfunctions showed relatively homogeneous sensitivity loss beyond the central field. Mid-peripheral dysfunction was a later feature; finally, only central and peripheral islands remained. Colocalized measures of visual function and retinal structure by OCT showed that visual function was detectable when a photoreceptor layer was detectable.

CONCLUSIONS—Residual rod as well as cone function is detectable in *RPE65*-LCA. The finding of different regional patterns of visual loss in these patients suggests that the optimal retinal site(s) for subretinal gene delivery to achieve efficacy are likely to change with disease progression.

Leber congenital amaurosis (LCA) is a molecularly heterogeneous group of autosomal recessive diseases with early onset of severe visual loss.[1] One molecular form of LCA is due to mutations in the gene encoding RPE65 (retinal pigment epithelium-specific 65 kDa protein). Scientific interest in RPE65 is high because this molecule is the long-sought isomerohydrolase of the visual cycle.[2–4] Medical interest has also been piqued by proof-of-concept experiments

Corresponding author: Samuel G. Jacobson, Scheie Eye Institute, University of Pennsylvania, 51 N. 39th Street, Philadelphia, PA 19104; jacobsos@mail.med.upenn.edu.

Disclosure: **S.G. Jacobson**, None; **T.S. Aleman**, None; **A.V. Cideciyan**, None; **A. J. Roman**, None; **A. Sumaroka**, None; **E.A.M. Windsor**, None; **S.B. Schwartz**, None; **E. Heon**, None; **E.M. Stone**, None

showing restored vision in two species of Rpe65-deficient animals by subretinal gene replacement therapy[5–10] and now in human clinical trials.[11–14]

Despite this remarkable progress, human *RPE65*-LCA disease remains incompletely understood. We know that severely impaired vision is associated with inheritance of two *RPE65* alleles which show little or no isomerohydrolase activity in vitro.[15] A visual toll is taken on both central and peripheral vision and on both rod and cone photoreceptor-mediated function (reviewed in Ref. 16). Unlike Rpe65-deficient animal models at early ages and stages, children with early visual dysfunction also have a serious retinal degeneration.[9,17,18] The retinal degeneration component tends to be masked by dysfunction resulting from the visual cycle abnormality, but eventually there is clinically apparent pigmentary retinopathy and chorioretinal atrophy.[16] Adding to the complexity is the fact that the visual cycle blockade in humans and animals is obviously not complete, because there is residual vision. Animal models with Rpe65 deficiency have residual photoreceptor function.[5,6,19–21] In mutant mice, the residual function has been ascribed to either low levels of production of 11-*cis*-retinal or Rpe65-independent pathways.[21,22]

The goal of the present study was to determine quantitatively key features of the residual vision in a population of patients with *RPE65*-LCA. We inquired whether the residual function was only cone- or also rod-mediated by using electroretinography (ERG) and full-field sensitivity testing (FST). The pattern of visual loss across the retina was explored with kinetic and dark-adapted static perimetry. The results have implications, not only for understanding the human disease but also for enhancing strategies for therapy of *RPE65*-LCA.

MATERIALS AND METHODS

Subjects

There were 30 patients (age range, 4–55) with *RPE65* mutations, representing 26 families (Table 1). Also included were data from an 8-year-old patient with autosomal dominant retinitis pigmentosa (adRP) caused by a rhodopsin (*RHO*) gene mutation. Normal subjects ($n = 16$; age range, 20–61) were also included. All patients with RPE65-LCA had a history of poor vision and nystagmus from infancy. A complete ophthalmic examination and visual function studies were performed (Table 1). Informed consent and assent were obtained; procedures adhered to the guidelines in the Declaration of Helsinki and were approved by the institutional review board.

Psychophysical Testing

Full-field stimulus testing (FST) was performed as previously described.[25,26] In brief, dark-adapted sensitivity to a full-field stimulus was measured in patients with *RPE65*-LCA ($n = 22$; age range, 5–46) using white, red, or blue flashes (200-ms duration) delivered with an LED-based, computer-driven stimulator (Colordome; Diagnosys LLC, Littleton, MA), and followed published procedures.[26] The white stimulus was used to quantify the level of sensitivity. FST loss was defined as the difference between mean normal and patient FST sensitivity. The sensitivity difference (blue-red) to chromatic stimulation was used to evaluate whether rods, cones, or both photoreceptor systems mediate perception. Cone-mediated perception is expected to yield nearly equal sensitivity values (blue-red difference, <3.1 dB) for both colors. Rod-mediated perception would yield a blue-red difference >19.3 dB. Values between those limits indicate that rods are mediating blue detection and cones are mediating red (mixed mediation).[25] Small differences in sensitivity peaks between rhodopsin and isorhodopsin[22] are not expected to be discernible by the FST method.

Kinetic perimetry was performed with targets V-4e and I-4e; the V-4e results were quantified with published methods.[27] Dark-adapted static threshold perimetry was performed with a modified automated perimeter (Humphrey Field Analyzer; Carl Zeiss Meditec Inc, Dublin, CA) and achromatic (white) stimuli (1.7° diameter; 200-ms duration) presented in a 12° grid across the visual field (71 extrafoveal locations).[28] It is important to note that the maximum intensity of the white stimulus from this automated perimeter is 1 log unit higher than that of the kinetic perimeter. An average of additional measurements performed at fixation and in a 4° grid centered at fixation was used as a sensitivity estimate for the most central location, which is plotted as a single value at 0° eccentricity. Psychophysical thresholds were also measured at 2° intervals spanning 60° along the horizontal and vertical meridians crossing fixation. Techniques, methods of data analysis and normal results have been described.[25,27,28] In a subset of patients (n = 13) and normal subjects (n = 4), dark-adapted sensitivity was plotted as a function of eccentricity in each subject. For central locations (within 10°) the data were obtained from horizontal sensitivity profiles with greater spatial resolution (see above). Sensitivity values at equal eccentricities were averaged.

Electroretinography

Full-field electroretinograms (ERGs) were performed in 29 patients with a standard protocol. Details of the methods and normal results have been published.[27,29] Reproducibility of small-amplitude flicker waveforms was validated by comparing several independent recordings.[30] In four patients, high-energy stimuli from a custom-built xenon flash stimulator (luminance of unattenuated white flash, 3.4 log cd · s · m^{-2}; duration: ~1 ms) were used to attempt to record ERG photoresponses under dark-adapted conditions. Details of the methodology and normal results have been published.[31,32]

Optical Coherence Tomography (OCT)

Cross-sectional retinal reflectivity profiles were obtained with OCT in 20 patients by using one of two instruments (OCT3 [Humphrey Instruments; Carl Zeiss Meditec, Inc.], with a resolution of ~8 μm (n = 6 patients), and the RTVue-100 (n = 14) [Optovue Inc., Fremont, CA], with a 5-μm axial resolution in tissue). Details of our recording and analysis techniques have been published.[18,23,33,34] Retinal cross sections were sampled with vertical scan groups centered on the anatomic fovea and consisting of five overlapping segments of linear scans, each 4.5 mm in length, extending 9 mm in either direction. Each segment was repeated at least three times. A video fundus image showing the location of the scanned segment was acquired and saved with each OCT scan by the commercial software. Post-acquisition processing of OCT data was performed with custom programs written in commercial software (MatLab 6.5; MathWorks, Natick, MA). Longitudinal reflectivity profiles (LRPs) making up the OCT scans were aligned by using a dynamic cross-correlation algorithm.[33] A manual override was used when crossing structures which interrupted local lateral isotropy by shadowing deeper signals. Nuclear layers were defined as previously published.[9,33,34] The outer photoreceptor nuclear layer (ONL) thickness was defined as the major intraretinal signal trough delimited by the signal slope maxima. ONL thickness was related to colocalized psychophysical thresholds determined by dark-adapted static perimetry along the same retinal regions. ONL thickness values were laterally averaged at 0.6-mm intervals to correspond with the lateral sampling of vision. For analysis pairs of colocalized measures of ONL thickness-sensitivity data from all patients were binned at 10-μm thickness intervals. ONL thickness values ≤5 μm were considered not detectable (ND).

RESULTS

Residual Function in RPE65 Deficiency: Cones, Rods, or Both

ERGs were abnormal in all patients with *RPE65*-LCA tested. There were no detectable waveforms in 41% of the patients tested, and the other 59% had signals to only some stimuli (described later). Representative ERGs in *RPE65*-LCA were compared with normal waveforms and those from a disease with primary rod dysfunction, autosomal dominant retinitis pigmentosa (adRP) caused by rhodopsin (*RHO*) gene mutation (Fig. 1A). The normal ERG to a dim blue light flash in the dark-adapted state represents a rod-mediated b-wave. A white light flash, dark-adapted, elicits a faster and larger waveform with both rod and cone (i.e., mixed) contributions, but is rod dominated. Cone ERGs are recordable in the light-adapted state to single flashes of light or to flickering light at 29 Hz. Severe early-onset rod disease and residual (but abnormal) cone function is exemplified by an 8-year-old patient with adRP who had the R135L *RHO* mutation. There was no measurable rod b-wave and, unlike the normal, waveforms elicited with white light stimuli in the dark- and light-adapted states were similar in shape and magnitude. There was a retained but abnormal flicker signal.

None of the patients with *RPE65*-LCA showed ERG responses to the dim blue light stimuli that normally evoke rod b-waves (Fig. 1A). Twelve patients (P1, P2, P13, P16, P19, P22, P23, P25–P28, and P30) had no detectable ERGs to any stimuli; eight patients (P5, P7, P8, P11, P15, P18, P21, and P24) had only small amplitude (range, 2–4 μV) flicker ERGs; and nine patients (P3, P4, P6, P9, P10, P12, P14, P17, and P20) showed similar responses to dark- and light-adapted white stimuli and flicker waveforms with amplitudes ranging from 4 to 35 μV (normal mean ± SD = 172 ± 35 μV). We also used bright flashes to elicit ERGs in four patients (P5, P17, P18, and P22); there were no detectable responses (data not shown). In summary, the detectable ERGs in *RPE65*-LCA showed the pattern of a retinopathy with such severe rod dysfunction that it is not detectable with this technique; residual and abnormal cone function were measurable in many of the patients.

FST was performed in 22 patients with *RPE65*-LCA by using white and chromatic stimuli (Fig. 1B). Sensitivity to the white stimulus in the patients with *RPE65*-LCA was abnormally reduced and showed a range of results representing sensitivity losses of 34 to 69 dB (Fig. 1B, left). Chromatic measurements showed that more than half of the patients (13/22; 59%; age range, 6–27 years; mean age, 16) had rod mediation of the blue stimulus, indicating that there was severely reduced but detectable residual rod function. The remaining patients (9/22; 41%; age range, 5–46 years; mean age, 24) detected both red and blue stimuli with cone-mediated vision (Fig. 1B, right). It can be concluded that residual rod function (and not only cone function) is detectable by psychophysics in patients with *RPE65*-LCA. There was no clear relationship of patient age to presence of residual rod function.

Localization of Residual Vision in the Visual Field

Kinetic visual fields with V-4e, a large bright target, were measurable in 29 of 30 patients. None of the patients was able to detect I-4e, the small bright target. A normal extent of kinetic field (defined as ≥90% for V-4e[27]) was present in four patients (P8, P12, P14, and P20) at ages 10, 12, 19, and 23, respectively; there were no absolute scotomas detectable within these fields. The kinetic field of P20 at age 23 (Fig. 2A, top left) exemplifies this pattern. Other patients (n = 13; age range, 4–33 years) showed sizeable fields that were generally constricted and had reduced extent (39%–88% of normal). Such patterns are exemplified by P3 at age 6 (Fig. 2A, top center). Later stage patterns showed either a residual central island, with or without peripheral islands, or only a far peripheral island (Fig. 2A, right: P24, age 29; P27, age 41; P23, age 28). The graph of these data indicates a wide variation in the extent of kinetic field

in the first two decades of life. Only islands of vision of limited extent were measurable after the third decade of life.

Limited longitudinal data for kinetic fields are also plotted (Fig. 2A) and illustrated (Figs. 2B–D). P8, at age 10 had a full kinetic field (to the V-4e target), but over the ensuing 11 years showed progressive loss of superior and then mid-peripheral fields; at age 21 there was a central island isolated by an absolute scotoma from a temporal peripheral island (Fig. 2B). P5, at age 10, had generalized constriction of field (39% of normal) and a follow-up at age 17 years revealed only a small central island (Fig. 2C). P18, at age 21, showed generalized constriction (38% of normal); at age 24, there was a residual central island with a temporal peripheral island (Fig. 2D).

Static threshold perimetry in the dark-adapted state was performed in 17 of the patients. The highest intensity of the white stimulus used in the static perimetry is 1 log unit higher than that in the kinetic perimeter. Maps of dark-adapted sensitivity are shown for normal subjects (mean map of four individuals; age range, 22–61 years) compared with results from eight representative patients with *RPE65*-LCA. Patients are ordered (left to right in each row) by their mean sensitivity across the field. P14 and P20 had the highest mean sensitivities among the eight patients shown; however, these dark-adapted sensitivities were still approximately 5 log units reduced compared with those of normal subjects (mean normal average, 72 dB [SD, 1.6] versus 23 and 19.1 dB, respectively, for P14 and P20). The sensitivity map for P20 shows some decrement in peripheral sensitivity with relative central and mid-peripheral field preservation. Other dark-adapted sensitivity maps (P11, P8, and P17) show losses in the mid-peripheral field but with residual islands of central and peripheral function. More advanced stages (P21, P13, and P23) show extensive mid-peripheral scotomas separating central from peripheral vision. It is of interest that patients at advanced disease stages with only central islands by kinetic perimetry ($n = 4$) all showed detectable peripheral islands by dark-adapted static perimetry. The peripheral islands were equal or lower in sensitivity than the central islands. A patient with retained peripheral function but no measurable central function by kinetic perimetry (P23), had measurable central and peripheral islands with dark-adapted static perimetry and there was greater sensitivity in the periphery. Such findings are most likely attributable to the 1-log-unit brighter stimulus available with the static perimeter.

Dark-adapted perimetry results were summarized by plotting sensitivity as a function of eccentricity, and these cross-sectional data were grouped to arrive at a hypothetical severity sequence of residual visual loss (Fig. 3B). These data support the notion that widespread loss of sensitivity occurs early in the disease and may progress to patchy loss, which then increases in severity. In normal subjects, sensitivity minimum is at fixation; there is an increase to a peak at ~12°; and a gradual decline occurs at greater eccentricities. Sensitivity in patients with *RPE65*-LCA was abnormally reduced at fixation but was still higher than at greater eccentricities, which were at least 4 log units reduced. The different patterns of loss at eccentricities >10° suggest a sequence of severity. At early stages (data from four patients, Fig. 3B, top right), there were relatively homogeneous losses between ~10° and the periphery. Later stages showed prominent losses between 30° and 60° eccentricity, and these regional mid-peripheral losses deepened while function nearer fixation declined less dramatically (data from five patients, Fig. 3B, lower left). The pattern at even later stages (data from four patients, Fig. 3B, lower right) suggested that the 30° to 60° region of loss had become an absolute scotoma; the extent of this scotoma was greater than at the previous stage and involved more central field. Data from four of these patients of comparable age (19–23 years) were used to illustrate further the hypothesized sequence of residual vision loss in *RPE65*-LCA (Fig. 3C). Relatively homogenous loss (P14) was followed by prominent mid-peripheral loss (P8) that can result in an absolute mid-peripheral scotoma (P21); finally, there was centripetal movement of the defect boundary and only central and/or peripheral islands of vision remained (P13).

Relation of Residual Vision to Residual Photoreceptor Structure

Visual function and retinal structure in *RPE65*-LCA are related in a complex manner because of dual defects that can affect vision in this disease: a biochemical blockade of the visual cycle and a complicating retinal degenerative process leading to photoreceptor cell loss.[9,18,24] We asked the practical question of whether detectable dark-adapted sensitivity to the white stimulus of the static perimeter had any relationship to the presence of measurable photoreceptor layer (outer nuclear layer, ONL). The answer to this question could be of value in screening candidate patients for therapy and in directing local therapy to appropriate retinal regions, especially those regions in the peripheral retina where large deviations from the optical axis result in loss of signal on OCT scans due to optical distortions.

Vertical cross-sectional OCT images of the retina spanning approximately 8 mm to either side of the fovea were analyzed in 20 patients with *RPE65*-LCA for ONL thickness (Fig. 4A). Vertical profiles of dark-adapted sensitivity were used to relate the presence or absence of visual sensitivity to ONL across this same region. Like the normal subject, P10 at age 12 had detectable visual sensitivity across the vertical meridian. There was a wide extent of measurable ONL (highlighted in blue on scans), although it was substantially reduced in thickness compared with normal. P22 at age 27, had ONL that extended from the fovea to approximately 3 to 4 mm superior and inferior; discontinuous with this ONL was a thinned segment of ONL detectable superiorly. Visual sensitivity was present in most of the region that showed detectable ONL.

To summarize the data in the 20 patients with *RPE65*-LCA, we sampled 487 loci along the vertical meridian for ONL thickness and detectable dark-adapted visual sensitivity (Fig. 4B). There were 95 loci with no measurable vision; 71 of these loci (75%) also had no measurable ONL. The remaining 24 loci with no vision had <135 μm of ONL thickness (mean, 8 μm [SD, 3.5]). Among the 392 loci with detectable dark-adapted visual sensitivity, 377 (96%) loci showed measurable ONL (mean, 21 μm [SD, 15]). The conclusion from these data representing a wide central retinal region is that presence of dark-adapted visual sensitivity is highly likely to be associated with the presence of underlying ONL.

DISCUSSION

Patients with RPE65-LCA in this study and in earlier reports (reviewed in Ref. 16) have markedly decreased but residual vision. The consensus from previous studies is that the limited residual function is cone mediated. The present study provides evidence of residual rod as well as cone vision in patients with *RPE65*-LCA; residual rod function has been reported in studies of Rpe65-deficient mice.[19,22,35] What is the biochemical basis of any residual vision in *RPE65*-LCA? The most parsimonious answer is that function represents residual *RPE65* activity from hypomorphic alleles (i.e., those with reduced but not absent levels of gene activity). In vitro analyses of some of the *RPE65* mutant alleles found in patients have indicated that isomerization activity may not be completely lost, suggesting partial function of the visual cycle in vivo.[15,36,37] Consistent with this notion is a report of a relatively mild form of *RPE65*-LCA in a patient with a mutant allele and in vitro evidence of higher residual levels of RPE65 activity.[38] Further, the *Rpe65 R91W* knock-in mice, unlike *Rpe65*$^{-/-}$, have measurable RPE65 and 11-*cis*-retinal.[21] There remains the possibility, however, that there are alternative RPE65-independent pathways that supply chromophore and are the basis of residual vision. For example, in *Rpe65*$^{-/-}$ mice, there is no measurable 11-cis retinal but definite residual retinal function.[19] It has been determined that 9-*cis* retinal can accumulate and the rod visual pigment isorhodopsin formed.[22] The exact source of the 9-*cis*-retinal is unknown, but the level is increased in *Rpe65*$^{-/-}$ mice that are dark reared or have decreased melanin levels.[39] Regeneration of chromophore in cones has long been considered to involve alternative RPE65-independent pathways in addition to the conventional RPE65-dependent visual cycle.[4,17,40]

Patterns of progressive loss of residual vision in *RPE65*-LCA were estimated with cross-sectional data from kinetic and dark-adapted static perimetry. All patients have at least 3 to 4 log units reduction of sensitivity to light, the presumed consequence of the visual cycle blockade from RPE65 deficiency. If the insensitivity was uniform across the retina, a simple model would predict a sensitivity versus eccentricity plot that resembled the normal (Fig. 3B, upper left) but one that was uniformly reduced by several log units. None of the patients in this study showed exactly this pattern. The mildest pattern did show a relatively slow decline in sensitivities >10°, which resembled the slow decline at these eccentricities in the normal plot. However, these patients also had prominent decreases in sensitivity between fixation and ~10°. From earlier studies of *RPE65*-LCA, we know that superimposed on an early-onset biochemical dysfunction is a component of retinal degeneration.[9,17,18,41] Already in the first decade of life, there are cone and rod photoreceptor losses, as demonstrated by measurement of ONL at the fovea and across the central 30° of retina.[17,18] The more central visual losses may at least partly be related to the topography of ONL thinning.[17,18] It is of interest that the mid-peripheral losses in sensitivity mimic patterns of visual field loss in forms of RP, many of which are known to be primary photoreceptor diseases. Late stage patterns with only residual central and peripheral islands are also a common finding in advanced RP.[42] The patterns of residual vision we observed may be partly due to underlying patterns of photoreceptor degeneration, especially at later disease stages. A component of scattered light from stimuli falling on severely degenerate retina may be extending some of the detected islands of vision. Adding further complexity is the possibility that human *RPE65*-LCA may undergo different rates of cone and rod degeneration, as in murine Rpe65 deficiency.[43]

Our evidence that ONL structure in a wide central region of retina generally follows the residual function, as measured with higher intensity dark-adapted static thresholds, leads to the speculation that such visual data may be usable as a surrogate measure for underlying photoreceptors. The practical implication of this result relates to ongoing clinical trials of gene therapy in *RPE65*-LCA.[11–14] The subretinal treatment zone in two of the three clinical trials has been mainly macular.[11,12] There is not yet any proof of efficacy in terms of foveal visual acuity and the occurrence of a complicating macular hole certainly indicates that foveomacular injections carry some increased complication risks.[12] We suggest that perifoveal or mid-peripheral subretinal injection sites be considered as alternate targets for gene therapy based on our recent OCT studies[17,18] and the present results indicating mid-peripheral preservation of residual sensitivity at relatively early disease stages. For patients at later disease stages, the choices become limited. These patients may be relegated to a category of ineligible for participation in gene therapy trials. Alternatively, if regions in their peripheral retina are functioning, it may be worth considering such patients for treatment. The only way to determine the value of this approach may be to perform peripheral retinal gene therapy in these patients. Such regions are less accessible to OCT because large deviations from the optical axis during imaging cause distortions and loss of signal. With the goal of enhancing orientation and mobility in patients who would not be strong candidates for more centrally located focal treatment, we propose that retained temporal peripheral vision responding to dark-adapted high intensity stimuli should be considered as an eligibility criterion for gene therapy in the nasal retina. The concept may be generalizable in the future for treatment of the many forms of RP with retained peripheral visual islands.

Acknowledgments

Supported by the Macula Vision Research Foundation, Hope for Vision, The Foundation Fighting Blindness, the Chatlos Foundation, the Ruth and Milton Steinbach Fund, Research to Prevent Blindness, and National Institutes of Health/National Eye Institute Grant U10-EY017280.

References

1. Stone EM. Leber congenital amaurosis: a model for efficient genetic testing of heterogeneous disorders: LXIV Edward Jackson Memorial Lecture. Am J Ophthalmol 2007;144(6):791–811. [PubMed: 17964524]
2. Moiseyev G, Chen Y, Takahashi Y, Wu BX, Ma JX. RPE65 is the isomerohydrolase in the retinoid visual cycle. Proc Natl Acad Sci USA 2005;102(35):12413–12418. [PubMed: 16116091]
3. Jin M, Li S, Moghrabi WN, Sun H, Travis GH. Rpe65 is the retinoid isomerase in bovine retinal pigment epithelium. Cell 2005;122(3):449–459. [PubMed: 16096063]
4. Travis GH, Golczak M, Moise AR, Palczewski K. Diseases caused by defects in the visual cycle: retinoids as potential therapeutic agents. Annu Rev Pharmacol Toxicol 2007;47:469–512. [PubMed: 16968212]
5. Acland GM, Aguirre GD, Ray J, et al. Gene therapy restores vision in a canine model of childhood blindness. Nat Genet 2001;28(1):92–95. [PubMed: 11326284]
6. Acland GM, Aguirre GD, Bennett J, et al. Long-term restoration of rod and cone vision by single dose rAAV-mediated gene transfer to the retina in a canine model of childhood blindness. Mol Ther 2005;12 (6):1072–1082. [PubMed: 16226919]
7. Narfström K, Katz ML, Bragadottir R, et al. Functional and structural recovery of the retina after gene therapy in the RPE65 null mutation dog. Invest Ophthalmol Vis Sci 2003;44(4):1663–1672. [PubMed: 12657607]
8. Dejneka NS, Surace EM, Aleman TS, et al. In utero gene therapy rescues vision in a murine model of congenital blindness. Mol Ther 2004;9(2):182–188. [PubMed: 14759802]
9. Jacobson SG, Aleman TS, Cideciyan AV, et al. Identifying photoreceptors in blind eyes caused by RPE65 mutations: prerequisite for human gene therapy success. Proc Natl Acad Sci USA 2005;102 (17):6177–6182. [PubMed: 15837919]
10. Pang JJ, Chang B, Kumar A, et al. Gene therapy restores vision-dependent behavior as well as retinal structure and function in a mouse model of RPE65 Leber congenital amaurosis. Mol Ther 2006;13 (3):565–572. [PubMed: 16223604]
11. Bainbridge JW, Smith AJ, Barker SS, et al. Effect of gene therapy on visual function in Leber's congenital amaurosis. N Engl J Med 2008;358(21):2231–2239. [PubMed: 18441371]
12. Maguire AM, Simonelli F, Pierce EA, et al. Safety and efficacy of gene transfer for Leber's congenital amaurosis. N Engl J Med 2008;358(21):2240–2248. [PubMed: 18441370]
13. Hauswirth WW, Aleman TS, Kaushal S, et al. Treatment of Leber congenital amaurosis by ocular subretinal injection of adeno-asso-ciated virus gene vector: short-term results of a phase 1 trial. Hum Gene Ther 2008;19:979–990. [PubMed: 18774912]
14. Cideciyan AV, Aleman TS, Boye SL, et al. Human gene therapy for RPE65 isomerase deficiency activates the retinoid cycle of vision but with slow rod kinetics. Proc Natl Acad Sci USA 2008;105 (39):15112–15117. [PubMed: 18809924]
15. Redmond TM, Poliakov E, Yu S, Tsai JY, Lu Z, Gentleman S. Mutation in key residues of RPE65 abolishes its enzymatic role as isomerohydrolase in the visual cycle. Proc Natl Acad Sci USA 2005;102(38):13658–13663. [PubMed: 16150724]
16. Paunescu K, Wabbels B, Preising MN, Lorenz B. Longitudinal and cross-sectional study of patients with early-onset severe retinal dystrophy associated with RPE65 mutations. Graefes Arch Clin Exp Ophthalmol 2005;243(5):417–426. [PubMed: 15565294]
17. Jacobson SG, Aleman TS, Cideciyan AV, et al. Human cone photoreceptor dependence on RPE65 isomerase. Proc Natl Acad Sci USA 2007;104(38):15123–15128. [PubMed: 17848510]
18. Jacobson SG, Cideciyan AV, Aleman TS, et al. Photoreceptor layer topography in children with Leber congenital amaurosis caused by RPE65 mutations. Invest Ophthalmol Vis Sci 2008;49(10):4573–4577. [PubMed: 18539930]
19. Van Hooser JP, Aleman TS, He YG, et al. Rapid restoration of visual pigment and function with oral retinoid in a mouse model of childhood blindness. Proc Natl Acad Sci USA 2000;97(15):8623–8628. [PubMed: 10869443]

20. Pang JJ, Chang B, Hawes NL, et al. Retinal degeneration 12 (rd12): a new, spontaneously arising mouse model for human Leber congenital amaurosis (LCA). Mol Vis 2005;11:152–162. [PubMed: 15765048]
21. Samardzija M, von Lintig J, Tanimoto N, et al. R91W mutation in Rpe65 leads to milder early-onset retinal dystrophy due to the generation of low levels of 11-cis-retinal. Hum Mol Genet 2008;17(2): 281–292. [PubMed: 17933883]
22. Fan J, Rohrer B, Moiseyev G, Ma JX, Crouch RK. Isorhodopsin rather than rhodopsin mediates rod function in RPE65 knock-out mice. Proc Natl Acad Sci USA 2003;100(23):13662–13667. [PubMed: 14578454]
23. Jacobson SG, Cideciyan AV, Aleman TS, et al. Crumbs homolog 1 (CRB1) mutations result in a thick human retina with abnormal lamination. Hum Mol Genet 2003;12(9):1073–1078. [PubMed: 12700176]
24. Jacobson SG, Cideciyan AV, Aleman TS, et al. RDH12 and RPE65, visual cycle genes causing Leber congenital amaurosis, differ in disease expression. Invest Ophthalmol Vis Sci 2007;48(1):332–338. [PubMed: 17197551]
25. Roman AJ, Schwartz SB, Aleman TS, et al. Quantifying rod photo-receptor-mediated vision in retinal degenerations: dark-adapted thresholds as outcome measures. Exp Eye Res 2005;80(2):259–272. [PubMed: 15670804]
26. Roman AJ, Cideciyan AV, Aleman TS, Jacobson SG. Full-field stimulus testing (FST) to quantify visual perception in severely blind candidates for treatment trials. Physiol Meas 2007;28(8):N51–N56. [PubMed: 17664667]
27. Jacobson SG, Yagasaki K, Feuer W, Roman AJ. Interocular asymmetry of visual function in heterozygotes of X-linked retinitis pigmentosa. Exp Eye Res 1989;48(5):670–691.
28. Jacobson SG, Voigt WJ, Parel JM, et al. Automated light- and dark-adapted perimetry for evaluating retinitis pigmentosa. Ophthalmology 1986;93(12):1604–1611. [PubMed: 3808619]
29. Aleman TS, Cideciyan AV, Volpe NJ, Stevanin G, Brice A, Jacobson SG. Spinocerebellar ataxia type 7 (SCA7) shows a cone-rod dystrophy phenotype. Exp Eye Res 2002;74(6):737–745. [PubMed: 12126946]
30. Jacobson SG, Buraczynska M, Milam AH, et al. Disease expression in X-linked retinitis pigmentosa caused by a putative null mutation in the RPGR gene. Invest Ophthalmol Vis Sci 1997;38(10):1983–1997. [PubMed: 9331262]
31. Cideciyan AV, Jacobson SG. An alternative phototransduction model for human rod and cone ERG a-waves: normal parameters and variation with age. Vision Res 1996;36(16):2609–2621. [PubMed: 8917821]
32. Cideciyan AV. In vivo assessment of photoreceptor function in human diseases caused by photoreceptor-specific gene mutations. Methods Enzymol 2000;316:611–626. [PubMed: 10800705]
33. Huang Y, Cideciyan AV, Papastergiou GI, et al. Relation of optical coherence tomography to microanatomy in normal and rd chickens. Invest Ophthalmol Vis Sci 1998;39(12):2405–2416. [PubMed: 9804149]
34. Jacobson SG, Sumaroka A, Aleman TS, et al. Nuclear receptor NR2E3 gene mutations distort human retinal laminar architecture and cause an unusual degeneration. Hum Mol Genet 2004;13(17):1893–1902. [PubMed: 15229190]
35. Seeliger MW, Grimm C, Ståhlberg F, et al. New views on RPE65 deficiency: the rod system is the source of vision in a mouse model of Leber congenital amaurosis. Nat Genet 2001;29(l):70–74. [PubMed: 11528395]
36. Chen Y, Moiseyev G, Takahashi Y, Ma JX. Impacts of two point mutations of RPE65 from Leber's congenital amaurosis on the stability, subcellular localization and isomerohydrolase activity of RPE65. FEBS Lett 2006;580(17):4200–4204. [PubMed: 16828753]
37. Takahashi Y, Chen Y, Moiseyev G, Ma JX. Two point mutations of RPE65 from patients with retinal dystrophies decrease the stability of RPE65 protein and abolish its isomerohydrolase activity. J Biol Chem 2006;281(31):21820–21826. [PubMed: 16754667]
38. Lorenz B, Poliakov E, Schambeck M, Friedburg C, Preising MN, Redmond TM. A novel RPE65 hypomorph expands the clinical phenotype of RPE65 mutations. Invest Ophthalmol Vis Sci 2008;49 (12):5235–5242. [PubMed: 18599565]

39. Fan J, Wu BX, Sarna T, Rohrer B, Redmond TM, Crouch RK. 9-cis retinal increased in retina of RPE65 knockout mice with decrease in coat pigmentation. Photochem Photobiol 2006;82(6):1461–1467. [PubMed: 16553465]

40. Schonthaler HB, Lampert JM, Isken A, et al. Evidence for RPE65-independent vision in the cone-dominated zebrafish retina. Eur J Neurosci 2007;26(7):1940–1949. [PubMed: 17868371]

41. Porto FB, Perrault I, Hicks D, et al. Prenatal human ocular degeneration occurs in Leber's congenital amaurosis (LCA2). J Gene Med 2002;4(4):390–396. [PubMed: 12124981]

42. Grover S, Fishman GA, Brown J Jr. Patterns of visual field progression in patients with retinitis pigmentosa. Ophthalmology 1998;105(6):1069–1075. [PubMed: 9627658]

43. Znoiko SL, Rohrer B, Lu K, Lohr HR, Crouch RK, Ma JX. Down-regulation of cone-specific gene expression and degeneration of cone photoreceptors in the Rpe65$^{-/-}$ mouse at early ages. Invest Ophthalmol Vis Sci 2005;46(4):1473–1479. [PubMed: 15790918]

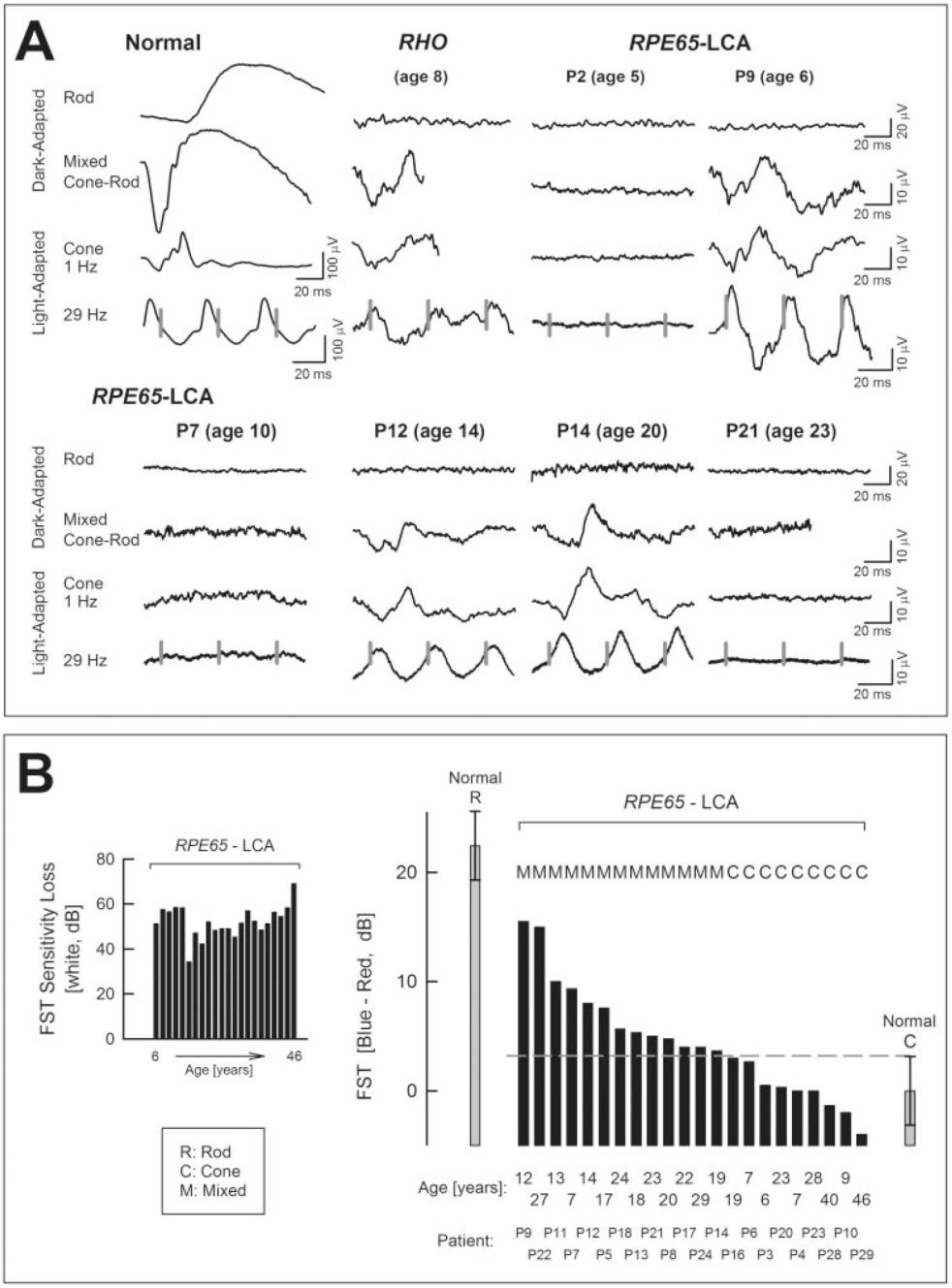

FIGURE 1.

Measures of residual function in *RPE65*-LCA. (**A**) Standard ERGs in patients with *RPE65*-LCA. Rod, mixed cone-rod, and cone ERGs from six representative patients with *RPE65*-LCA (age range, 5–23 years) were compared with ERGs of a patient with a *rhodopsin* (*R135L*) gene mutation showing residual, severely abnormal, cone-mediated function. A normal subject (age 20 years) is shown for comparison (*left*). Traces start at stimulus onset; calibrations are to the *right* and *below* waveforms. ERGs can be undetectable, even at early ages. Detectable ERGs show a pattern similar to that of the patient with a *RHO* mutation and severe rod dysfunction but residual and abnormal cone function. (**B**) *Inset* (*left*): FST sensitivity loss to a white stimulus in patients with *RPE65*-LCA ranked by age. Chromatic FST sensitivity differences (blue-red)

in patients with *RPE65*-LCA ranked in decreasing order of magnitude (*right*). Results in normal subjects in the dark-adapted state (*left*) or at the cone plateau of dark-adaptation after light-exposure (*right*) served to define which photoreceptor mediates perception of each color (error bars, mean ± 2 SD). Labels above the bars denote photoreceptor mediation: R, rods; M, mixed; C, cones. Ages of the patients and their numbers are shown *below* each bar on the horizontal axis. *Dashed line*: delimits the upper limit for categorization as cone-mediated.

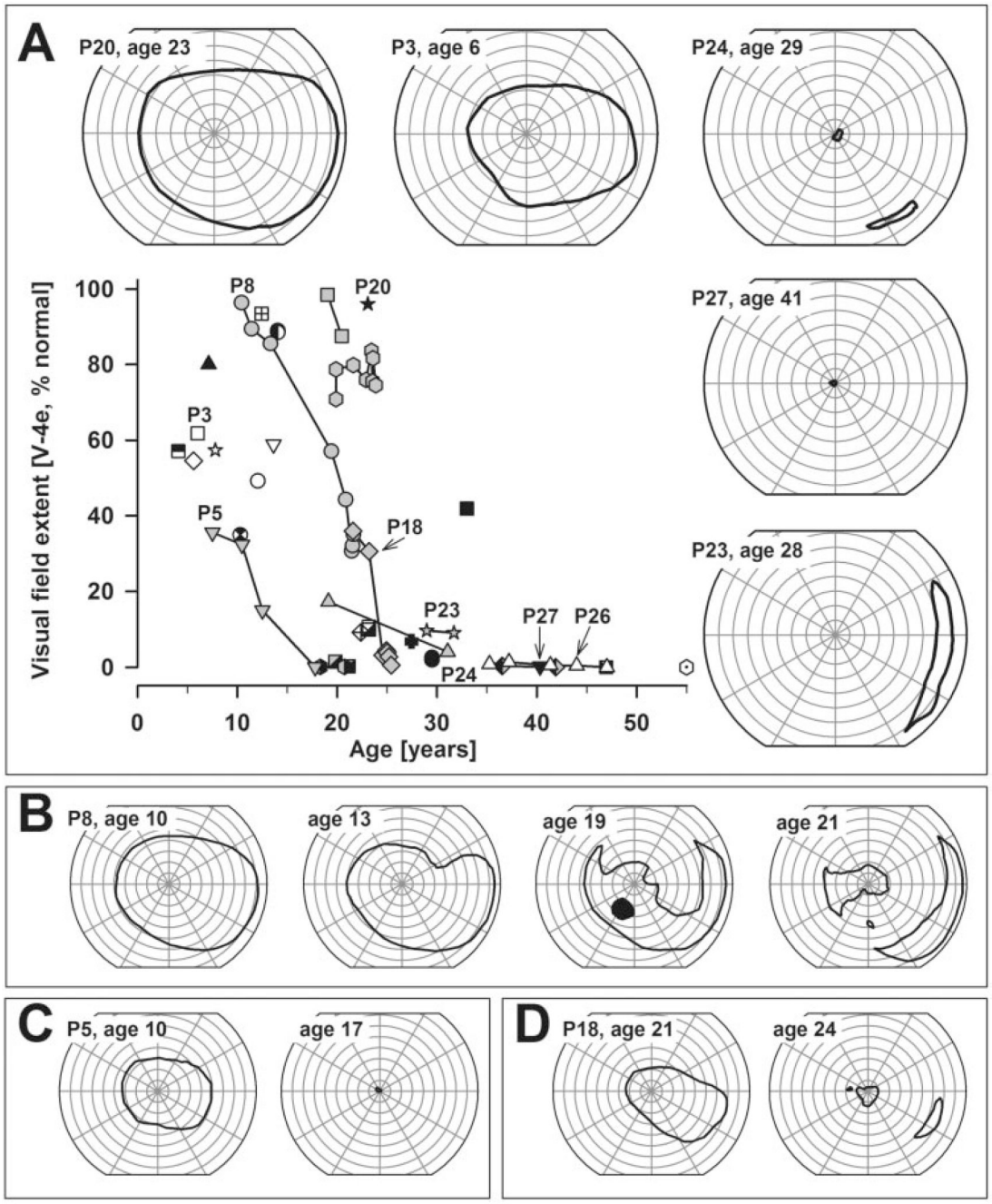

FIGURE 2.

Kinetic perimetry in *RPE65*-LCA. (**A**) Kinetic field extent expressed as a percentage of normal and plotted as a function of age of patient. Longitudinal data are connected by lines. Representative kinetic fields illustrating early and later stage patterns are shown (*above* and to the *right* of the graph). All fields are depicted as right eyes. (**B–D**) Serial kinetic fields in one eye of three patients spanning 11 years in P8 (**B**), 7 years in P5 (**C**), and 3 years in P18 (**D**). Patients with illustrated visual fields are identified in (**A**).

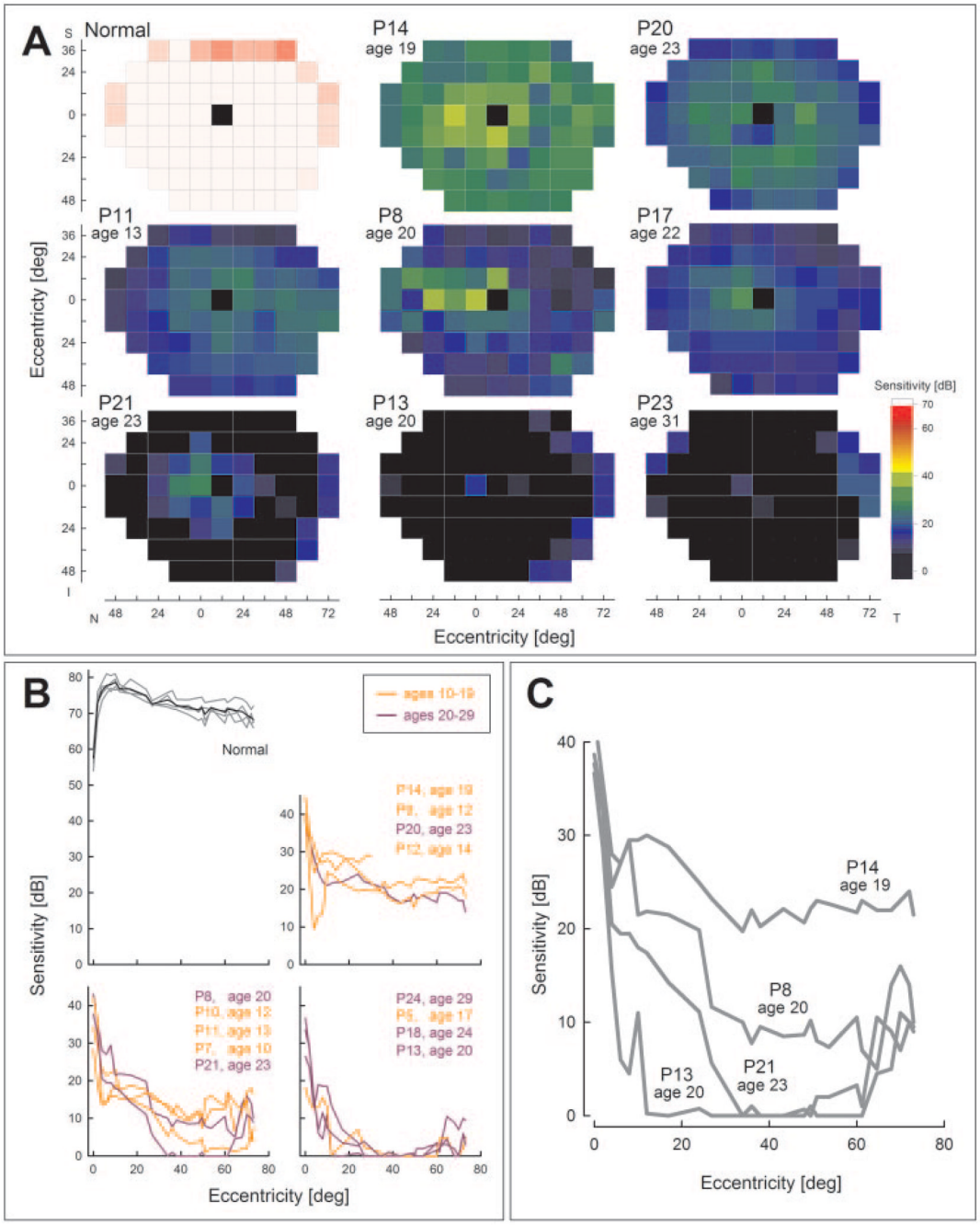

FIGURE 3.

Dark-adapted static threshold perimetry to a white stimulus in *RPE65*-LCA. (**A**) Sensitivities at 71 loci in normal subjects (N) and patients with *RPE65*-LCA are mapped to a pseudocolor scale representing 7 log units. Eight patient sensitivity maps are shown and ordered (*left* to *right* in each of three rows) by mean sensitivity calculated across the field. All data are depicted as right eyes to enable comparison. The normal blind spot is shown as a *black square* at the 12° temporal field. (**B**) Sensitivity as a function of eccentricity in patients with *RPE65*-LCA compared with normal subjects (*top left*). Patients are grouped by increasing severity of sensitivity loss (from *top right* to *lower left* to *lower right*; and within panels from *top* to *bottom*). Data traces are colored to show the two decades of ages represented (*orange*, 10–19

years; *purple*, 20–29 years). (**C**) Data from four patients of comparable age (19–23 years) that illustrate further the patterns of increasing severity.

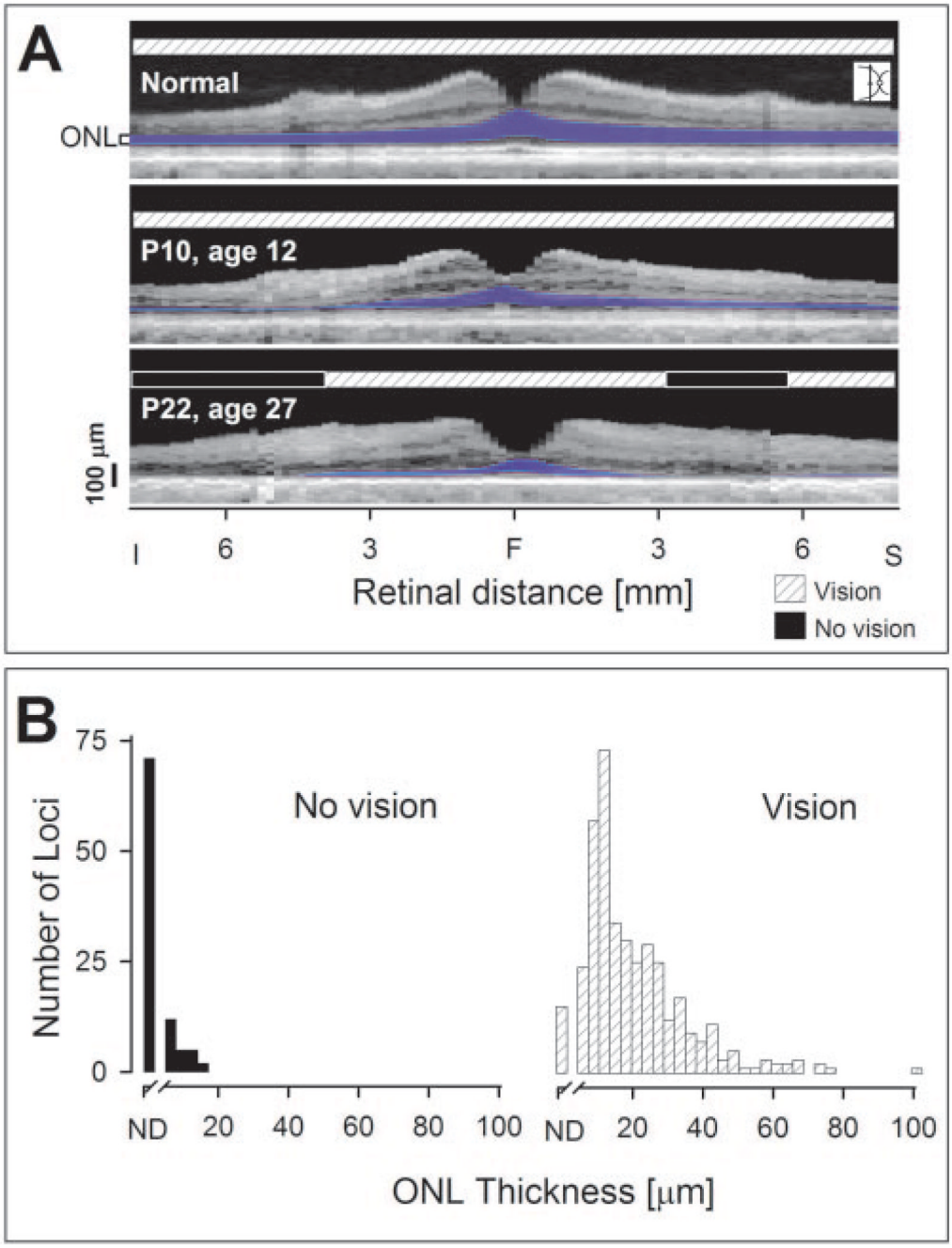

FIGURE 4.

Relationship between dark-adapted visual function and retinal structure in *RPE65*-LCA. (**A**) Vertical cross-sectional retinal images using OCT compared with the presence or absence of visual response in corresponding locations. A 48-year-old normal subject and two patients with *RPE65*-LCA (P10, P22) are compared. Each patient shows a different degree of ONL preservation (highlighted in *blue* on scan). Apparent peaks at the vitreoretinal surface at ~4 to 5 mm eccentricity along some of these vertical scans are the nerve fiber layer bundles and arcade vessels. (**B**) Summary of data from 487 loci along the vertical meridian in 20 patients.

ONL thickness is plotted for loci with absence (*left*, 95 loci) or presence (*right*, 392 loci) of dark-adapted visual sensitivity.

TABLE 1

Molecular and Clinical Characteristics of the *RPE65*-LCA Patients

Patient	Age at First Visit (y)/ Sex	Ethnicity	Mutations	Visual Acuity (RE-LE)*	Fundus Features)†	Ages at Follow-up Visits (y)	Reference‡
P1§	4/M	Indian	A500del5bp/A500del5bp	20/100		—	17
P2§	5/F	Indian	A500del5bp/A500del5bp	20/125		—	17
P3‖	6/M	Indian	R44Q/R44Q	20/63		—	17, 18
P4	7/F	Black	R91W/R91W	20/63	¶	—	17, 18
P5	7/F	Hispanic	97del20bp/97del20bp	20/160		10, 12, 17	9, 17, 18, 23, 24
P6‖	7/M	Indian	R44Q/R44Q	20/160		—	17, 18
P7#	7/M	Hispanic	L341S/IVS2–2A>C	20/100–20/200		10	18
P8	10/M	Caucasian	Y368H/Y368H	20/160–20/100		11, 13, 19, 20, 21	9, 17, 23
P9	6/F	Black	L408P/L408P	20/80–20/50		12	17, 18
P10#	9/M	Hispanic	L341S/IVS2–2A>C	20/63–20/80		12	18
P11	13/F	Indian	V287F/V287F	20/125–20/200		—	17, 18
P12	14/F	Caucasian	R91Q/R91W	20/32–20/32		—	17, 18
P13	18/F	Hispanic	L341S/L341S	20/250–20/320		20,21	9, 17
P14	19/F	Caucasian	G40S/R91Q	20/320–20/400		20	17, 18, 24
P15**	19/F	Black-Indian	R91Q/IVS7+4A>G	20/400		31	17
P16	19/M	Black	R91W/R91W	20/200–20/800		21	17, 24
P17	19/F	White	R91W/R44Q	20/200–20/160		22, 23, 24	9, 17
P18	21/M	White	E417Q/E417Q	20/160		23,24,25	9, 17
P19**	22/M	Black-Indian	R91Q/IVS7+4A>G	20/200–20/70		—	This study
P20	23/M	Asian	R91W/1059_1060inslbp	20/60–20/40		—	17, 18, 24
P21	23/F	Caucasian	G104D/G40S	20/125–20/160	††	—	This study
P22	27/F	Asian	H182R/H182R	20/160–20/1600			9, 17
P23	28/F	Caucasian	Y368H/297dellbp	LP		31	9, 17
P24	29/M	Caucasian	H182Y/G40S	20/800–20/640	††, ‡‡	—	This study
P25	33/F	Caucasian	IVS1 + 5G>A/W460X	20/1600–20/800		—	This study
P26	35/M	Caucasian	IVS1 + 5G>A homoallelic	20/1600–20/800	††, ‡‡	37,41,44,47	9, 17

Patient	Age at First Visit (y)/ Sex	Ethnicity	Mutations	Visual Acuity (RE-LE)*	Fundus Features)†	Ages at Follow-up Visits (y)	Reference‡
P27	36/M	Caucasian	Y144D/Y144D	20/200	‡‡	41	9, 17
P28	40/F	Caucasian	K303X/Y431C	HM-20/1600	‡‡	—	9, 17
P29	46/F	Caucasian	Y239D/Y368H	LP	‡‡	—	This study
P30	55/M	Caucasian	A132T/A132T	LP	††, ‡‡	—	This study

HM, hand motion; LP, light perception

*Best corrected visual acuity; similar in the two eyes unless specified.

†All patients had vessel attenuation and most (except P1-P4, P6, and P7) had the appearance of RPE depigmentation and granularity in the fundus. Less universal features are indicated: ¶, fine white dots; ††, moderate bone spicule-like pigment; ‡‡, macular atrophic changes.

‡Previous reports of genotype and/or phenotype by the authors.

§, ‖, #, **Patients are siblings.